forests

MDPI

Article

A Novel GIS-Based Random Forest Machine Algorithm for the Spatial Prediction of Shallow Landslide Susceptibility

Viet-Hung Dang [1], Nhat-Duc Hoang [2], Le-Mai-Duyen Nguyen [3], Dieu Tien Bui [4] and Pijush Samui [5,6,*]

[1] Faculty of Information Technology, Duy Tan University, 03 Quang Trung, Da Nang 550000, Vietnam; dangviethungha@gmail.com
[2] Faculty of Civil Engineering, Institute of Research and Development, Duy Tan University, P809 - 03 Quang Trung, Danang 550000, Vietnam; hoangnhatduc@duytan.edu.vn
[3] Faculty of Electrical Engineering, Duy Tan University, 03 Quang Trung, Danang 550000, Vietnam; maiduyennl@gmail.com
[4] GIS Group, Department of Business and IT, University of South-Eastern Norway, Gullbringvegen 36, N-3800 Bø i Telemark, Norway; Dieu.T.Bui@usn.no
[5] Geographic Information Science Research Group, Ton Duc Thang University, Ho Chi Minh City 700000, Vietnam
[6] Faculty of Environment and Labour Safety, Ton Duc Thang University, Ho Chi Minh City 700000, Vietnam
* Correspondence: pijush.samui@tdtu.edu.vn

Received: 2 November 2019; Accepted: 14 January 2020; Published: 19 January 2020

Abstract: This study developed and verified a new hybrid machine learning model, named random forest machine (RFM), for the spatial prediction of shallow landslides. RFM is a hybridization of two state-of-the-art machine learning algorithms, random forest classifier (RFC) and support vector machine (SVM), in which RFC is used to generate subsets from training data and SVM is used to build decision functions for these subsets. To construct and verify the hybrid RFM model, a shallow landslide database of the Lang Son area (northern Vietnam) was prepared. The database consisted of 101 shallow landslide polygons and 14 conditioning factors. The relevance of these factors for shallow landslide susceptibility modeling was assessed using the ReliefF method. Experimental results pointed out that the proposed RFM can help to achieve the desired prediction with an F1 score of roughly 0.96. The performance of the RFM was better than those of benchmark approaches, including the SVM, RFC, and logistic regression. Thus, the newly developed RFM is a promising tool to help local authorities in shallow landslide hazard mitigations.

Keywords: random forest machine; landslide; geographic information system; machine learning; hybrid approach

1. Introduction

A landslide, which is defined as the slope movement of soil, mud, debris, or rock, is the most common geological hazard in the world [1]. This hazard happens as a consequence of other events or actions, such as torrential rain, earthquake, deforestation, or mineral exploitation. Globally, landslides have substantial social and economic impacts. Globally, during the 1995–2014 period, more than 3876 landslides occurred causing 163,658 deaths and 11,689 injuries [2].

Vietnam is one of the countries profoundly affected by landslides in Asia. According to the Institute of Geosciences and Mineral Resources in Vietnam, there are more than 10,200 locations that have a high risk of landslides in the northern mountainous provinces [3]. From 2000 to 2015, there

were 250 flash floods and landslides, with 779 people killed or going missing and 426 others injured. Therefore, being able to predict future landslides can assist with policy-making and development-planning and, as a result, can save lives and reduce economic damages through prevention and mitigation measures.

Landslide prediction can be built in the form of susceptibility maps where the likelihood of a future landslide occurring is given based on a set of local terrain conditions and geo-environmental factors [4]. Literature review shows that five main approaches are used for constructing landslide susceptibility, namely: (a) geomorphological mapping, (b) heuristic or index-based approaches, (c) analysis of landslide inventories, (d) physics-based methods, and (e) statistically-based methods. The first two approaches are qualitative methods [4]. In other words, they are subjective and present susceptibility levels in descriptive terms. They rely heavily on the researcher in charge. In geomorphological mapping, a direct method, the susceptibility map is built through evaluating and mapping the actual and potential slope failure [5–8]. In the heuristic approach, the researcher ranks and weights all the known instability factors based on their expert experience [9]. The last three approaches are indirect and quantitative. Analyses of landslide inventories use present and past landslides to predict the occurrence of future ones [10,11]. Physics-based methods, on the other hand, use simplified physical models to simulate and predict slope instability [12–14]. Lastly, statistically-based methods attempt to build the functional relationship between past landslides, present landslides, and some inferred conditioning factors [15–20].

Among these approaches, statistically-based methods are by far the most popular ones. According to [4], from January 1983 to June 2016, there were 565 peer-reviewed articles on statistically-based landslide susceptibility models. The popularity of these techniques include both classical ones, such as discriminant analysis, logistic regression [21–25], data overlay, multi-criteria decision evaluation, and machine-learning-based ones, such as artificial neural networks [26], neuro-fuzzy models [27], support vector machine [28], decision trees [29], and sophisticated hybrid or ensemble learning approaches [16,30–32].

Multiple factors determine the popularity of statistically-based methods. First, it is their use of natural characteristics that allow them to be used in many scenarios for different regions of interest [4]. Second, these methods have demonstrated their effectiveness for a wide range of applications, as reported in various previous works [33,34]. Third, with the introduction of GIS, spatial-temporal landslide data can be seamlessly integrated with data of multiple conditioning factors. This provides a perfect setting for statistically-based methods to be built.

With GIS, greater inferred instability factors, including the relationship between past and present landslides, are considered and these factors become more and more nonlinear. Consequently, traditional linear methods, such as linear discriminant analysis and linear/logistics regression, are not satisfactory. Since 2000, machine learning and artificial intelligence (MLAI) have become increasingly popular due to their ability to handle multiple governing factors and nonlinearity. Thus, MLAIs have proven their efficiency in the spatial prediction of various geoscience fields, such as atmospheric particulate matter [35], earth fissure [36], snow avalanche [37,38], multi-hazard exposure [39], groundwater [40], and flash flood [41,42]. In landslide studies, the most vital issue for the successful application of MLAI is the ability to generate probabilistic inferences, which are widely used for susceptibility indices. Following this success trend, new and advanced MLAI algorithms for landslide modeling have received much interest. This is because, despite their versatility, there is still no single algorithm that is the best for all study areas [43,44]. The effectiveness of MLAI algorithms can significantly depend not only on the characteristics of the considered study region but also on the data available.

In this work, we developed and proposed, for the first time, a novel hybridization of random forest classifier (RFC) and support vector machine (SVM), named random forest machine (RFM), for shallow landslide susceptibility prediction. The RFC model, also called a random decision forest classifier, was introduced initially by Ho [45] and, then, further developed by Breiman [46]. Whereas, the SVM model, developed by Vapnik and collaborators [47,48], is widely recognized as a powerful

and robust model in environmental modeling. It is noted that the application of individual RFC or SVM for landslide susceptibility studies has been widely carried out [25,49–51].

The critical advantage of RFC is to build a forest of tree predictors, where each predictor operates on a random subset of data. The final classification is developed to take into account the results of all the predictors. The SVM classifier, on the other hand, is a maximum-margin classifier, where hyper-planes are constructed to separate classes. To the best of our knowledge, no research on a combination of the two algorithms has been conducted. Thus, the novelty of our proposed hybrid method is that SVM builds decision functions by using sub-datasets generated by RFC. Then, support vectors are determined to maximize the margins between the training data and the classifying borders.

Consequently, smoother final borders were derived with lows for both the number of trees and the depth level of each tree. Furthermore, the proposed hybrid method also avoided the limitations of SVM when working with large training datasets. Herein, the model only fed their subsets and facilitated parallel model training. The rest of the paper is organized as follows: the second section provides a general description and inventory of the study area. The third section reviews the RFC and SVM algorithms. The combination of these two algorithms to build landslide susceptibility maps is explained in the fourth section, followed by the reported experimental results. The last section is devoted to the discussion of experimental results.

2. The Study Area and the Landslide Inventory

2.1. General Description of the Study Area

The city chosen was the capital city of Lang Son province in northern Vietnam. It is located between the longitudes of 106°41′34″ E and 106°48′32″ E, and between the latitudes of 21°49′43″ N and 21°57′13″ N. The study area was roughly 101.3 km^2, slightly larger than the official area of Lang Son city (see Figure 1). The elevation of the area ranges from 214 to 800 m, with an average of 325.6 m above standard sea level.

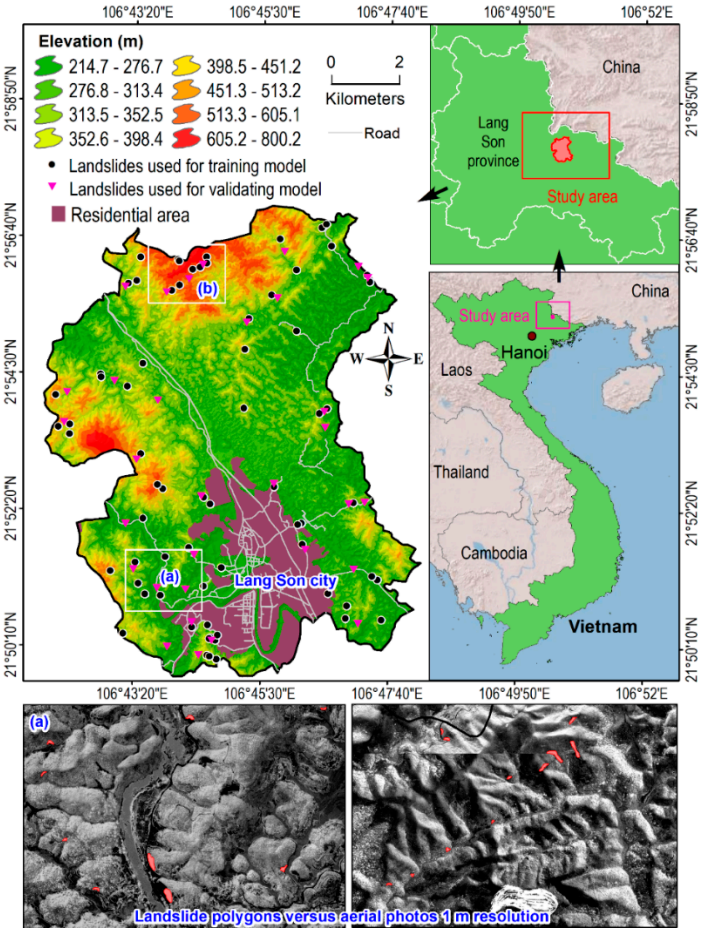

Figure 1. Location of the study area and landslide inventory.

The area has a strong northeastern-monsoon-influenced climate with high humidity (between 80% and 85%) and a high amount of rainfall (annually average from 1200 to 1600 mm). The rainy season is usually from May to September, but might last longer, up to 10 months. The area is relatively far from the sea and rarely on the direct path of tropical cyclones or tropical depressions. However, these extreme weather events can affect the weather of the region, causing prolonged torrential rains, which are the leading cause of landslides in the region, according to historical records.

2.2. Landslide Inventory Map

Information on past landslides in the area were collected to build the inventory map. We used different ways to obtain the necessary data. For landslides occurring before 2003, the locations were extracted from (1) field survey data with handheld GPSs and (2) one-meter resolution aerial photographs provided by the Vietnam Aerial Photography and Photogrammetry company [52]. For landslides that occurred in the period from 2003 to 2009, we got the locations from previous projects [53]. Lastly, for recent landslides, the locations were obtained from the field works of [32]. The inventory map contained only the information of rainfall-induced landslides, as there has never been a documented earthquake-induced landslide in the region. Few rockfall events were eliminated from the inventory as we were only interested in soil slides and debris flows.

In the final version of the inventory map (refer to Figure 1), there were 101 landslide polygons, which were split into two separate groups. Group 1 with 69 polygons was devoted to model training and group 2, consisting of 32 polygons, was employed for model validation. The total number of pixels of both groups was 3455, where 2410 pixels belonged to group 1 and 1045 pixels belonged to group 2. In order to have a complete data set, the GIS database was used to sample non-landslide locations.

2.3. Landslide Conditioning Factors

One of the few widely accepted principles in landslide prediction is that the conditioning factors that caused past and recent landslides will likely be the ones triggering future landslides [4]. Also, according to previous studies [54–56], a good selection of landslide conditioning factors is one of the vital requirements to have accurate landslide susceptibility maps. Based on an analysis performed by [32], other previous works [24,52], and the availability of data in the study region, 14 conditioning factors were chosen for this study. They included 10 geomorphometrical factors, namely, slope angle (SA), slope length (SL), slope aspect (SA), curvature (Curv.), elevation (Elev.), topographic wetness index (TWI), stream power index (SPI), sediment transport index (STI), valley depth (VD), toposhade (Topo.), and 4 geo-environmental factors, namely lithology (Lith.), land use (LU), soil type (ST), and distance to faults (DTF).

The geomorphometrical factors were derived from topographic maps at 1:5000 scale for the Lang Son city and 1:10,000 scale for the other study areas. These maps were derived from 1:20,000 scale aerial photos using the Imagestation Stereo Softcopy Kit software Version 2.3 (Intergraph Corporation, Huntsville, AL, USA). The intervals of contour lines were from 0.5 m for flat areas to 5 m for mountainous areas. First, a 5 m × 5 m digital elevation map (DEM) was generated from topographic maps. Then, ArcGIS 10.7.1 (ESRI Inc., Redlands, CA, USA) was utilized to obtain all the geomorphometrical factors using a raster resolution of 5 m. Jenks Natural Break optimization method [57] in ArcGIS 10.2 was employed to classify continuous-values factors (except slope aspect) into classes, as proposed by [58].

Regarding the four geo-environmental factors, lithology was obtained from four tiles of the Geological and Mineral Resources Map (GMRM) of Vietnam at a scale of 1:50,000. Soil type, on the other hand, was extracted from National Pedology Maps (NPM) at a scale of 1:100,000. Land use was obtained from a land use status map at scale 1:50,000 provided by the local authority. Lastly, distance to faults was constructed from the fault lines of the lithological data using ArcGIS 10.2. In summary, all 14 selected conditioning factors and their classes are summarized in Figure 2.

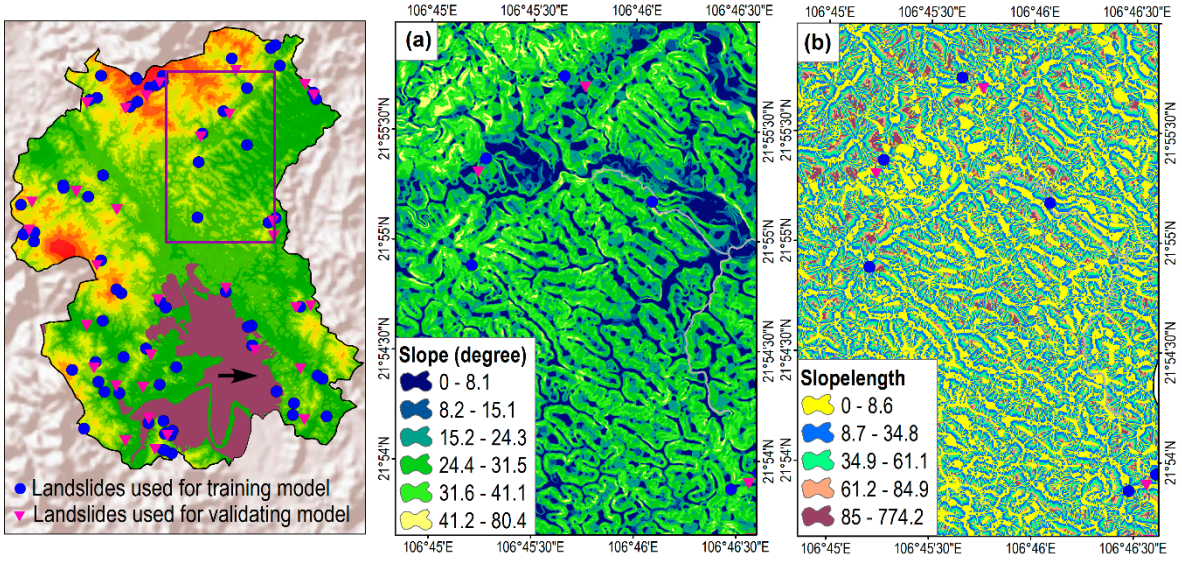

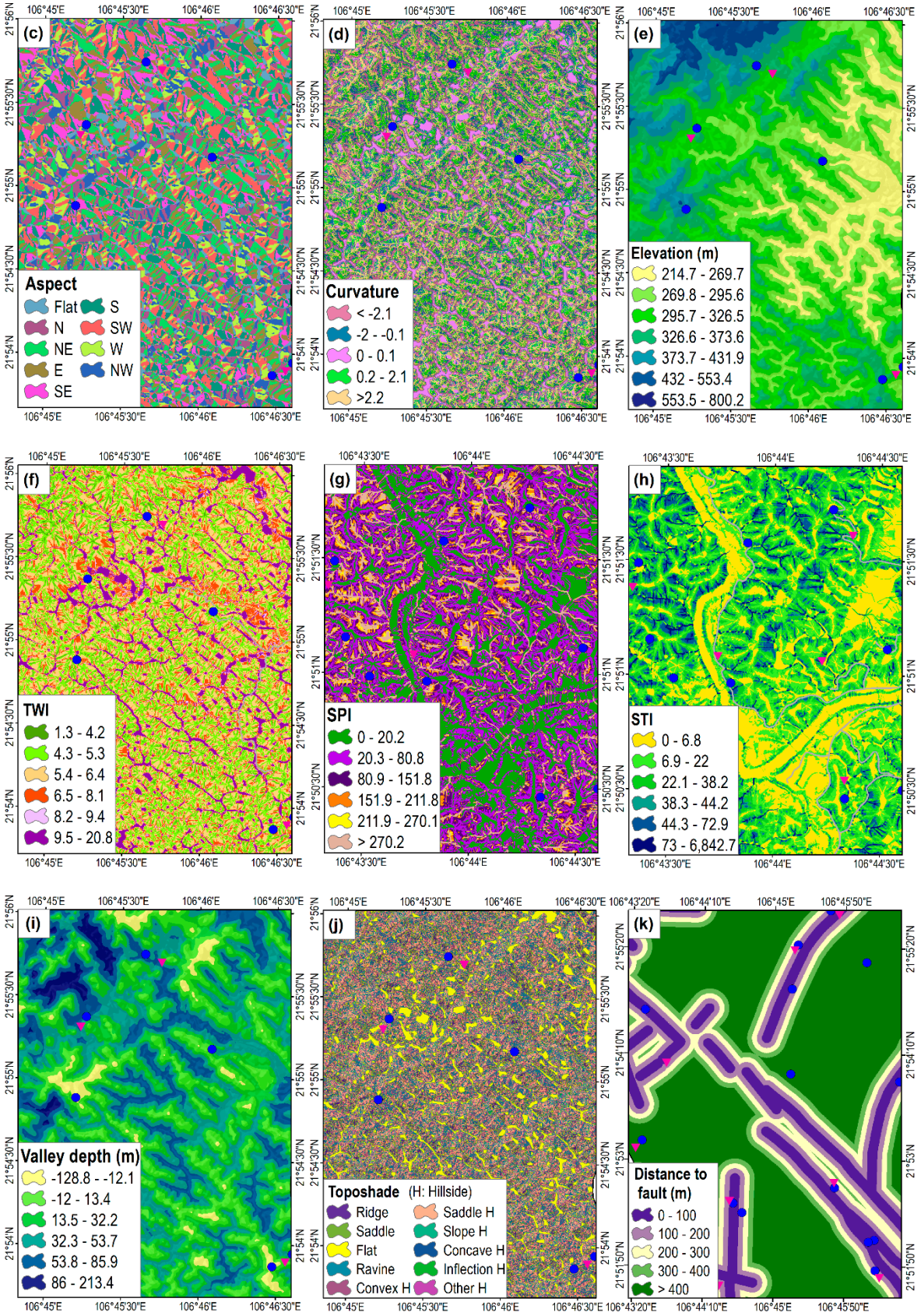
(c)
Aspect
Flat
S
N
SW
NE
W
E
NW
SE
(d)
Curvature
< -2.1
-2 - -0.1
0 - 0.1
0.2 - 2.1
>2.2
(e)
Elevation (m)
214.7 - 269.7
269.8 - 295.6
295.7 - 326.5
326.6 - 373.6
373.7 - 431.9
432 - 553.4
553.5 - 800.2
(f)
TWI
1.3 - 4.2
4.3 - 5.3
5.4 - 6.4
6.5 - 8.1
8.2 - 9.4
9.5 - 20.8
(g)
SPI
0 - 20.2
20.3 - 80.8
80.9 - 151.8
151.9 - 211.8
211.9 - 270.1
> 270.2
(h)
STI
0 - 6.8
6.9 - 22
22.1 - 38.2
38.3 - 44.2
44.3 - 72.9
73 - 6,842.7
(i)
Valley depth (m)
-128.8 - -12.1
-12 - 13.4
13.5 - 32.2
32.3 - 53.7
53.8 - 85.9
86 - 213.4
(j)
Toposhade (H: Hillside)
Ridge
Saddle H
Saddle
Slope H
Flat
Concave H
Ravine
Inflection H
Convex H
Other H
(k)
Distance to fault (m)
0 - 100
100 - 200
200 - 300
300 - 400
> 400

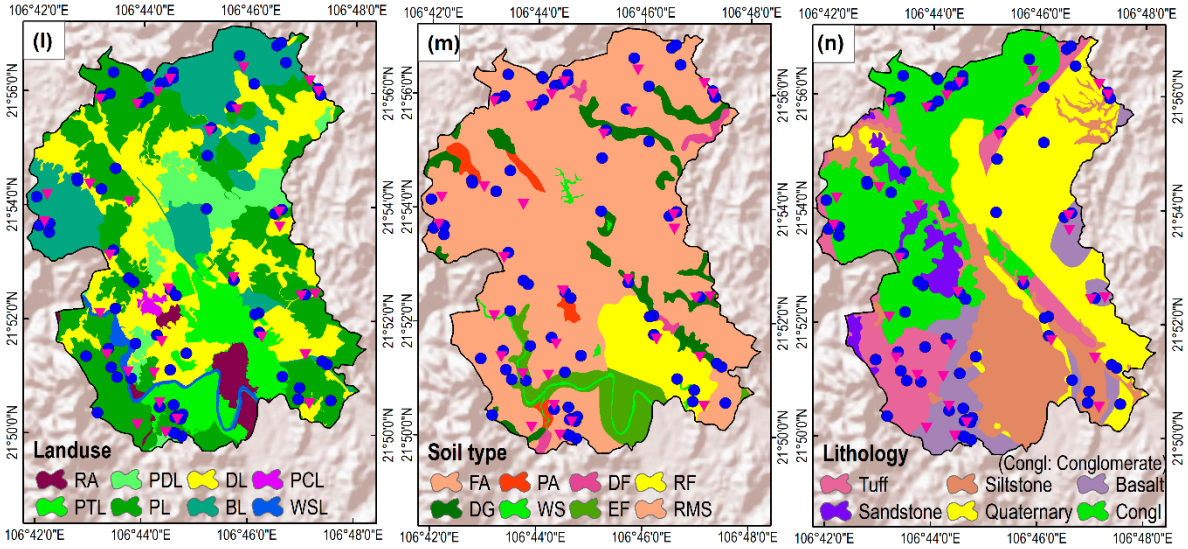

Figure 2. Landslide conditioning factors used in the study area: (**a**) slope, (**b**) slope lengths (**c**) aspect, (**d**) curvature, (**e**) elevation, (**f**) TWI (topographic wetness index), (**g**) SPI (stream power index), (**h**) STI (sediment transport index), (**i**) valley depth, (**j**) topo-shape, (**k**) distance to faults, (**l**) land use, (**m**) soil type, and (**n**) lithology. Explanations of land use and soil type can be found in [52].

2.4. Investigation on the Importance of the Landslide Conditioning Factors

Before the RFM model training phase commenced, it was necessary to inspect the relevancy of the collected variables used for landslide susceptibility mapping. In this study, the relevance of the influencing factors was preliminarily evaluated by the ReliefF method [59]. The ReliefF method is a probabilistic method used to inspect the conditional dependencies between variables and is capable of expressing the discriminative power of each variable used for data classification purposes. This method calculates a weight value for each variable to quantify its relevancy. A large weight is typically associated with an essential factor. The ReliefF analysis results are depicted in Figure 3. As can be seen from this figure, the slope was the most relevant factor for spatial mapping of landslide susceptibility in the study area, followed by SPI and elevation. Moreover, since all of the variable weights were not null, there was no redundant variable and all of them could be used for spatial mapping of landslide susceptibility.

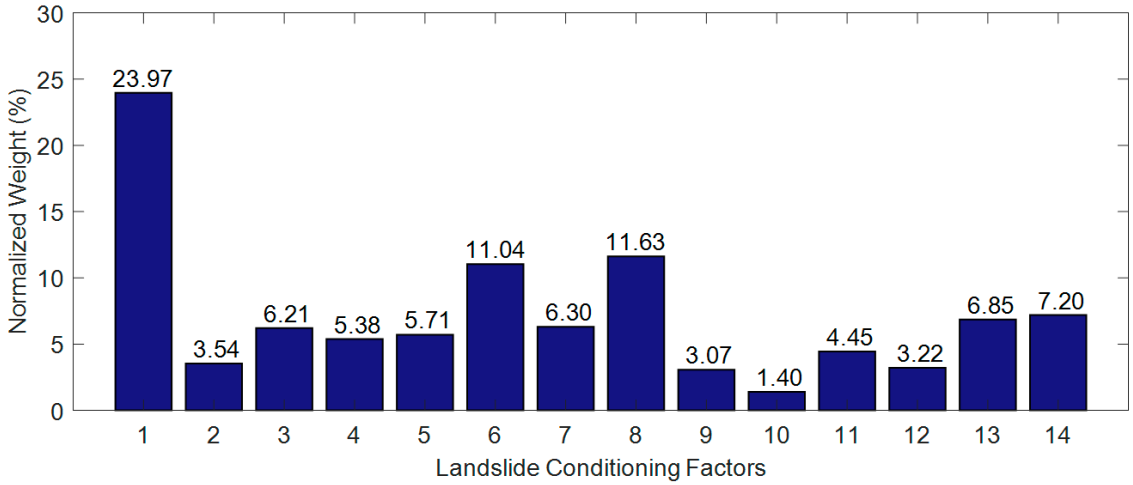

Figure 3. Variable analysis with the ReliefF method: (1)—Slope; (2)—Slope length; (3)—Aspect; (4)—Curvature; (5)—Elevation; (6)—TWI; (7)—SPI; (8)—STI; (9)—Valley depth; (10)—Topo-shape; (11)—Distance to faults; (12)—Land use, (13)—Soil type; and (14)—Lithology).

3. Research Methodology

3.1. Random Forest Classifier

RFC is an effective decision tree ensemble used for large-scale and multivariate pattern recognition [60]. This ensemble learning is established based on the concept of the random subspace method [45] and the stochastic discrimination method of classification [61]. The RFC was then further extended by Breiman [46] who introduced the concept of bagging and random feature selection. Equipped with these features, a random forest model becomes a powerful tool to construct an ensemble of classification trees. Successfully applications of RFC have been reported in various studies [25,35,49,62–65], including landslide modeling [25,66,67]

Given a labeled data set (D) for training $D = (X, Y)$, in which $x_i \in X$ ($i = 1,2, \ldots, N$, where N is the number of training samples) is a data sample and $y_i \in Y$ is its class label, the RFC method aims at constructing a model, which is capable of separating the input space into different disjoint regions. Each of the regions is characterized by one class label. To achieve this goal, the method trains k individual decision trees, where each tree is associated with a random Θ_k vector, which represents a subspace of the original input space. Subsequently, a single tree k is constructed by sampling with replacement $n < N$ data samples from the original training set. An individual tree (h_k) is therefore expressed as:

$$h_k(X, \Theta_k) = Y \tag{1}$$

During the training phase of a decision tree, a node can be expanded with two children to enhance the data classification performance (see Figure 4). This process is characterized by a split cut at the corresponding d^{th} dimension of the input data. The decision tree algorithm selects the most suitable node using the Gini impurity index (G) product (P) [49]; this product is computed as follows:

$$P = G_1 G_2 \tag{2}$$

where a Gini impurity index (G) of set k is defined as follows [68]:

$$G_k = 1 - \sum_{i=1}^{n_{kc}} p_{ki}^2 \tag{3}$$

where n_{kc} represents the number of classes in the considered set and p_{ki} denotes the ratio of the present class i in this set.

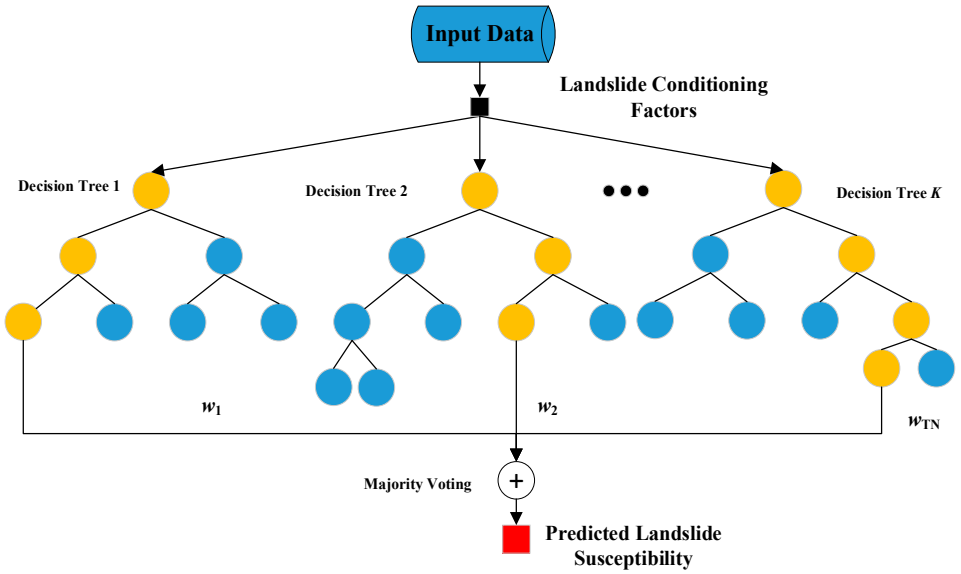

Figure 4. The general structure of the Random Forest Classifier (RFC) model in this research.

When a new input query is presented to the model, the RFC determines its output class through the majority vote standard [69]. Thus, the class label (y) of an input data x is computed from the established ensemble in the following manner:

$$y = H(x) = \underset{z}{argmax}\left(\sum_{k} I(h_k(x, \Theta_k) = z)\right) \quad (4)$$

where $I(t)$ denotes an indicator function defined as follows:

$$I(t) = \begin{cases} 1, & t \text{ is true} \\ 0, & t \text{ is false} \end{cases} \quad (5)$$

3.2. Support Vector Machine (SVM)

Support vector machine (SVM), proposed by Vapnik [47], is a powerful method for data classification, which is formulated on the basis of statistical learning theory. The main advantages of the SVM are the capability to deal with nonlinearly separable data, the ability to cope with multivariate data, resilience to noise, and the ability to avoid overfitting. The SVM deals with nonlinear datasets via the employment of kernel tricks. This machine learning method first maps the data from the original input space to a high-dimensional feature space within which a hyper-plane can be used to perform data classification (see Figure 5). An SVM-based model is also built on the concept of the maximum margin classifier, which is less sensitive to noise. Moreover, this machine learning is based on the concept of structural risk minimization, which can be resistant to overfitting. Due to such reasons, the SVM has been successfully employed for pattern recognition tasks in natural hazard mapping [37,70–73]. In landslide modeling, the SVM has been considered to be a standard method in susceptibility mapping and prediction [23,50,51,74,75].

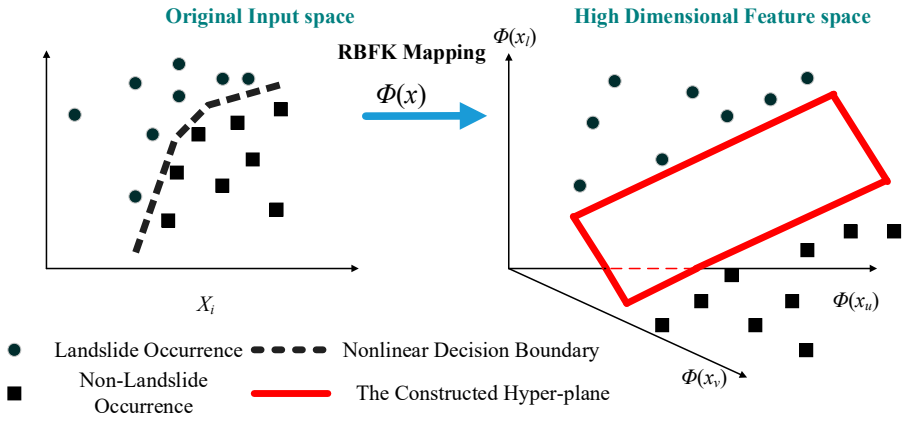

Figure 5. Illustration of the SVM based data classification (RBFK: Radial Basis Function Kernel).

Given a training dataset $(x_k, y_k)_{k=1}^{N}$ with input data $x_k \in R^n$ and corresponding class labels $y_k \in (-1, +1)$, the SVM model constructs a classification boundary from the training set so that the margin between the two classes is as wide as possible. Herein, the class output of −1 denoted a non-landslide occurrence and +1 represented a landslide occurrence.

The training phase of the SVM-based classification model boils down to solving the following constrained nonlinear programming [76]:

$$\text{Minimize } J_p(w, e) = \frac{1}{2} w^T w + c\frac{1}{2}\sum_{k=1}^{N} e_k^2, \quad (6)$$

$$\text{subjected to } y_k(w^T \varphi(x_k) + b) \geq 1 - e_k, k = 1, \ldots, N, e_k \geq 0, \quad (7)$$

where $w \in R^n$ denotes a normal vector to the classification hyper-plane; w^T is the transpose matrix of w; $b \in R$ denotes the model bias; $e_k > 0$ denotes slack variables; c denotes a penalty constant; $\varphi(x)$ is the aforementioned nonlinear data mapping; and $J_p(w, e)$ is the constrained nonlinear programming.

Another advantage of the SVM is that its training and prediction phase do not require the explicit expression of $\varphi(x)$. Alternatively, the algorithm only requires computing the product of $\varphi(x)$ in the input space, which is essentially a kernel function ($K(x_k, x_l)$) given by:

$$K(x_k, x_l) = \varphi(x_k)^T \varphi(x_l). \quad (8)$$

where x_l is the RBF center.

Moreover, the radial basis function kernel (RBFK) is often used in the SVM's training and prediction phases. The formulation of the RBFK is given by:

$$K(x_k, x_l) = exp(-\frac{\|x_k - x_l\|^2}{2\sigma^2}), \quad (9)$$

where σ denotes a tuning parameter, which can be determined via a grid search process [77].

Accordingly, the SVM model used for landslide susceptibility mapping can be presented as follows:

$$y(x_l) = sign(\sum_{k=1}^{SV} \alpha_k y_k K(x_k, x_l) + b), \quad (10)$$

where α_k is the solution of the dual form of the aforementioned nonlinear programming and *SV* denotes the number of support vectors (the number of $\alpha_k > 0$).

4. The Proposed Random Forest Machine (RFM) for GIS-Based Landslide Susceptibility Prediction

The overall structure of the proposed RFM model, which is a combination of the GIS database, RFC (random forest classifier) and SVM (support vector machine) algorithms is demonstrated in Figure 6. In order to construct the newly developed machine learning model for predicting a landslide, the GIS database of the studied region is first established. Accordingly, digital topographic maps, land use maps at a scale of 1:50,000, Landsat-8 Operational Land Imager (OLI) images with a resolution of 30 m, and geological data (e.g., lithology, soil type, and distance to fault) were utilized. In total, 101 landslide locations were identified and processed to formulate the GIS database for the study area. It was noted that all landslide conditioning variables were converted into a raster format with 5 m resolution utilizing a geospatial tool developed by the authors and opened in the ArcGIS software package.

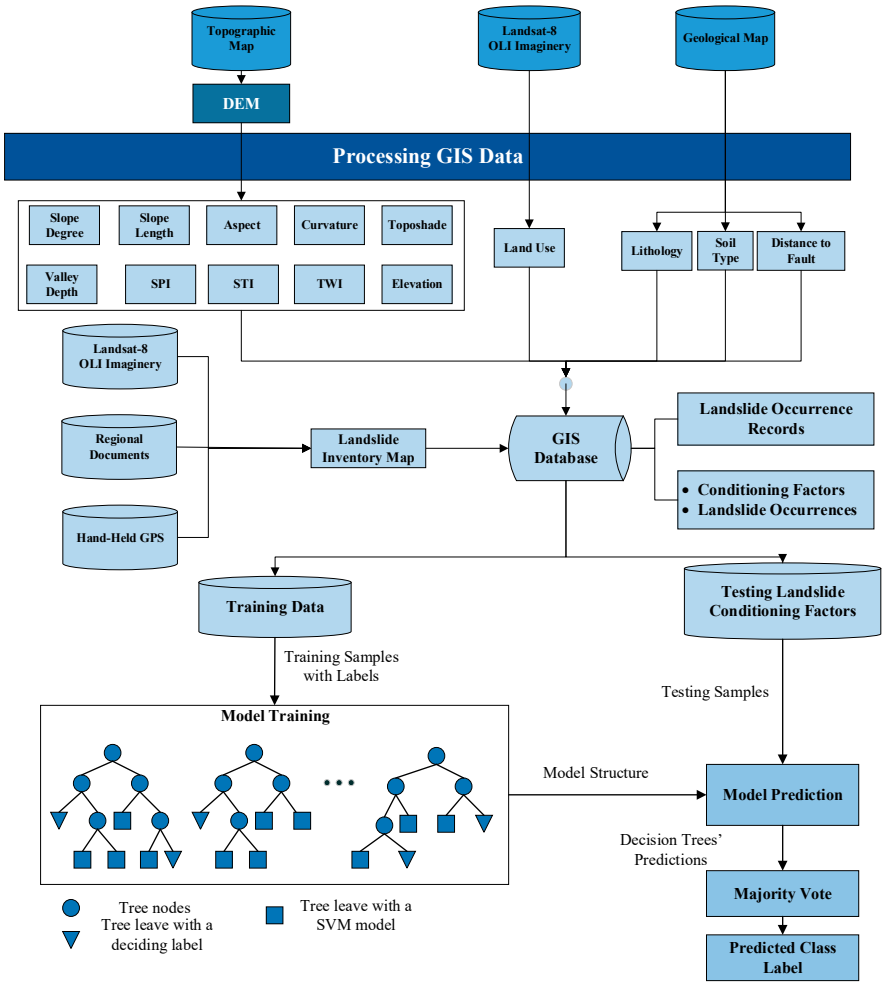

Figure 6. The GIS-based random forest machine for landslide susceptibility prediction.

Since the landslide susceptibility mapping was formulated as a supervised learning task, it was necessary to divide the whole collected data into training and testing datasets. The first set was used to construct the machine learning model, whereas the second set was reserved to verify the model's predictive performance. Thus, the whole dataset, consisting of 6910 samples (3455 landslide pixels and 3455 non-landslide points), was separated into the two subsets above within which the testing samples accounted for 30% of the data. The label of the dataset was encoded -1 for the negative class and +1 for the positive class. Moreover, the employed landslide conditioning factors were converted from categorical classes into continuous values within the range of 0.01 and 0.99 using a method described in Tien Bui et al. [78]. The purpose of this data conversion was to facilitate the subsequent pattern classification process.

Based on the collected GIS database, the RFM developed in this study was utilized as an intelligent data classification method to categorize the pixels into the positive class of landslide and the negative class of non-landslide. In the standard procedure of a decision tree, a model performs splitting operations at thresholds that are orthogonal to the axes of the input space (refer to Figure 7). The splitting regions were characterized by hyper-rectangles and the final decision borders had the form of linear functions parallel to the coordinate axes. The linear-decision borders undoubtedly limit the flexibility of the classifier and also necessitate a large number of individual trees to capture a complex decision surface. Therefore, this study proposed to combine SVM and RFC by adding SVM directly into the structure of individual trees.

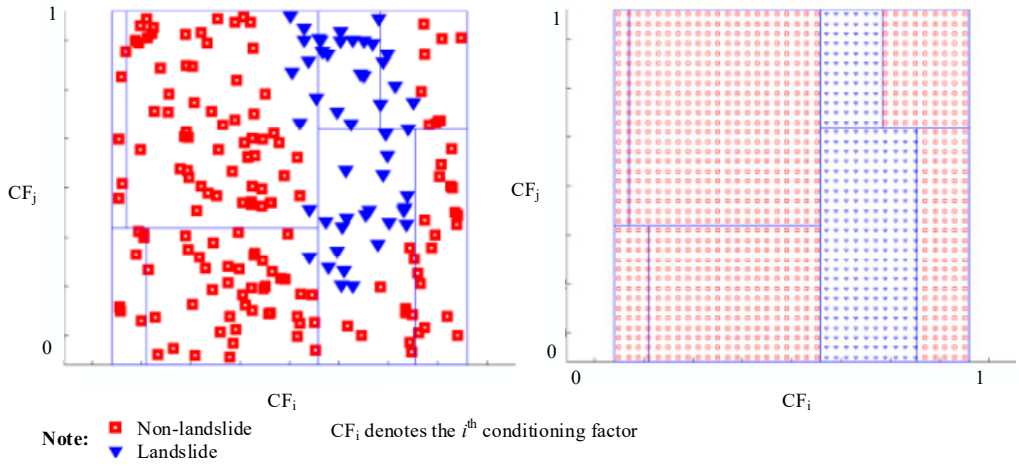

Figure 7. Illustrations of a complete training for a decision tree: (**a**) splitting thresholds and (**b**) the resulting decision border between classes.

Specifically, for each hyper rectangle, the SVM model was trained and its support vectors were identified. These support vectors helped to define the decision surface that maximizes the margins between the training data and the classifying borders. The direct outcome of this RFC-SVM integration was smooth final borders with a low number of trees and low levels on each tree (refer to Figure 8). Notably, another advantage of the proposed combined method was that it helps to overcome the limitations of SVM used for a large-scale training dataset where a vast kernel matrix must be computed because the whole dataset is divided into subsets by the RFC algorithm; thus, this helped to reduce the number of elements in the kernel matrices of the SVM models. The rules used to construct the RFM model were as follows (refer to Figure 6):

(i) If all the training data points in a node belong to the same class, then the node label is assigned as the data label;
(ii) If there are different labels in a node, the SVM structure is used to classify the data stored in this node.

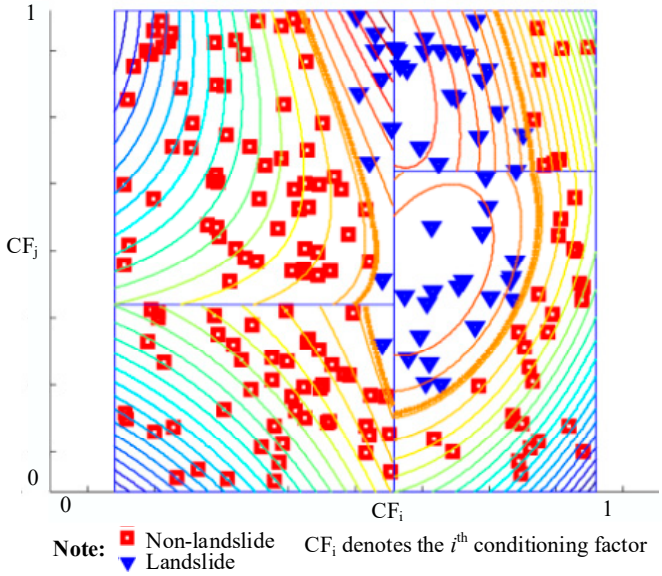

Figure 8. Illustration of using the SVM and the resulting smooth borders (bold curves).

Furthermore, to evaluate the RFM performance, the true positive rate (TPR; the percentage of positive instances correctly classified), the false positive rate (FPR; the percentage of negative instances misclassified), the false negative rate (FNR; the percentage of positive instances

misclassified), and the true negative rate (TNR; the percentage of negative instances correctly classified) can be used [52,66,79–81]. These indices are given by:

$$\text{TPR} = \frac{\text{TP}}{\text{TP+FN}}, \tag{11}$$

$$\text{FPR} = \frac{\text{FP}}{\text{FP+TN}}, \tag{12}$$

$$\text{FNR} = \frac{\text{FN}}{\text{TP+FN}}, \tag{13}$$

$$\text{TNR} = \frac{\text{TN}}{\text{TN+FP}}, \tag{14}$$

where *TP*, *TN*, *FP*, and *FN* are the true positive, true negative, false positive, and false negative, respectively.

Based on the aforementioned indices, the classification rate (CAR), precision, recall, and F1 score [82] can be calculated as follows:

$$\text{CAR} = \frac{\text{TP+TN}}{\text{TP+TN+FP+FN}}, \tag{15}$$

$$\text{Precision} = \frac{\text{TP}}{\text{TP+FP}}, \tag{16}$$

$$\text{Recall} = \frac{\text{TP}}{\text{TP+FN}}, \tag{17}$$

$$\text{F1 Score} = \frac{2\text{TP}}{2\text{TP+FP+FN}}. \tag{18}$$

It was noted that the goal of this study was to construct a landslide prediction model with good precision (low false positive outcomes) and recall (low false-negative outcomes) results. Therefore, this study assigned equal weighting values for precision and recall indices.

5. Experimental Results

This section presents the experimental results of the RFM model used for spatial landslide susceptibility mapping. As stated earlier, to train and test the model predictive capability, the original dataset was randomly divided into training (70%) and testing (30%) sets. Accordingly, the numbers of data samples (or pixels within the map of the study area) in the whole dataset, training, and testing sets were 3455, 2410, and 1045, respectively.

It was also noted that all 14 conditioning factors were used for spatial landslide modeling. Besides, to diminish the bias caused by randomness in the data sampling process, repeated sampling with 20 runs were performed. In each run, the training and testing datasets were extracted randomly from the collected dataset. The experimental outcomes of the proposed RFM model are reported in Table 1 and Table 2, including the mean and standard deviation (SD) of the performance measurement indices.

Table 1. Training performance of the RFM model.

Run No.	CAR	TPR	FPR	FNR	TNR	Precision	Recall	F1 score
1	0.965	0.945	0.013	0.055	0.987	0.988	0.945	0.966
2	0.969	0.949	0.009	0.051	0.991	0.991	0.949	0.970
3	0.969	0.951	0.012	0.049	0.988	0.989	0.951	0.970
4	0.965	0.944	0.012	0.056	0.988	0.989	0.944	0.966
5	0.967	0.948	0.013	0.052	0.987	0.988	0.948	0.968
6	0.966	0.945	0.012	0.055	0.988	0.988	0.945	0.966
7	0.967	0.949	0.012	0.051	0.988	0.989	0.949	0.969
8	0.965	0.946	0.014	0.054	0.986	0.986	0.946	0.966
9	0.969	0.950	0.011	0.050	0.989	0.990	0.950	0.970
10	0.963	0.941	0.013	0.059	0.987	0.988	0.941	0.964
11	0.969	0.949	0.010	0.051	0.990	0.990	0.949	0.969
12	0.967	0.947	0.012	0.053	0.988	0.988	0.947	0.967

13	0.966	0.945	0.010	0.055	0.990	0.990	0.945	0.967
14	0.967	0.948	0.011	0.052	0.989	0.990	0.948	0.969
15	0.966	0.945	0.011	0.055	0.989	0.990	0.945	0.967
16	0.969	0.952	0.012	0.048	0.988	0.988	0.952	0.970
17	0.968	0.948	0.010	0.052	0.990	0.991	0.948	0.969
18	0.965	0.946	0.015	0.054	0.985	0.986	0.946	0.966
19	0.967	0.946	0.012	0.054	0.988	0.988	0.946	0.967
20	0.968	0.949	0.012	0.051	0.988	0.989	0.949	0.969
Mean	0.967	0.947	0.012	0.053	0.988	0.989	0.947	0.968
SD	0.002	0.003	0.001	0.003	0.001	0.001	0.003	0.002

Table 2. Testing performance of the RFM model.

	CAR	**TPR**	**FPR**	**FNR**	**TNR**	**Precision**	**Recall**	**F1 score**
1	0.954	0.934	0.024	0.066	0.976	0.978	0.934	0.956
2	0.960	0.939	0.017	0.061	0.983	0.984	0.939	0.961
3	0.962	0.941	0.016	0.059	0.984	0.985	0.941	0.963
4	0.950	0.920	0.015	0.080	0.985	0.986	0.920	0.952
5	0.957	0.932	0.014	0.068	0.986	0.987	0.932	0.959
6	0.953	0.929	0.019	0.071	0.981	0.982	0.929	0.955
7	0.955	0.930	0.017	0.070	0.983	0.984	0.930	0.956
8	0.959	0.937	0.019	0.063	0.981	0.982	0.937	0.959
9	0.951	0.923	0.020	0.077	0.980	0.980	0.923	0.951
10	0.960	0.936	0.015	0.064	0.985	0.986	0.936	0.960
11	0.958	0.939	0.020	0.061	0.980	0.981	0.939	0.960
12	0.949	0.927	0.027	0.073	0.973	0.974	0.927	0.950
13	0.949	0.921	0.019	0.079	0.981	0.982	0.921	0.950
14	0.959	0.937	0.017	0.063	0.983	0.984	0.937	0.960
15	0.955	0.929	0.018	0.071	0.982	0.983	0.929	0.955
16	0.957	0.931	0.016	0.069	0.984	0.985	0.931	0.957
17	0.966	0.948	0.014	0.052	0.986	0.987	0.948	0.967
18	0.955	0.929	0.016	0.071	0.984	0.985	0.929	0.956
19	0.957	0.930	0.015	0.070	0.985	0.985	0.930	0.956
20	0.955	0.931	0.016	0.069	0.981	0.982	0.931	0.956
Mean	0.956	0.932	0.017	0.068	0.982	0.983	0.932	0.957
SD	0.004	0.007	0.003	0.007	0.003	0.003	0.007	0.004

Moreover, to confirm the predictive performance of the proposed RFM used for spatial mapping of landslide susceptibility in the study region, its predictive result was compared to those of the SVM, RFC, and stochastic gradient descent logistic regression (SGD-LR). All of the selected benchmark models have been employed for spatial prediction of landslide with good predictive performances [21,23,25,49–51,65,83]. The SVM and RFC models were implemented with the help of the MATLAB machine learning toolbox (Natick, MA, USA) [84]. The RFC was constructed with 100 individual decision trees. Besides, the SGD-LR was developed in the MATLAB environment by the authors. The prediction results of the proposed RFM, as well as other benchmark models, are summarized in Table 3 and Figure 9. As can be seen from this table, the average performance of the RFM (F1 score = 0.957) was better than those of the SVM (F1 score = 0.925), RFC (F1 score = 0.931), and SGD-LR (F1 score = 00.878). Also, the consuming time for runing the RFM, SVM, RFC, and SGD-LR models were 2.72, 2.66, 6.45, and 3.51 , respectively. This fact indicates that the proposed RFM, which was an integration of the RFC and SVM, is more computationally efficient than the RFC model. Besides, there was only a minor difference in computing time between the RFM and the individual SVM model.

Table 3. Prediction result comparison.

Phase	**Indices**	**The Proposed RFM**		**SVM**		**RFC**		**SGD-LR**	
		Mean	**Std**	**Mean**	**Std**	**Mean**	**Std**	**Mean**	**Std**
Training	CAR (%)	96.685	0.170	93.042	0.247	94.172	0.276	87.461	0.290
	TPR	0.947	0.003	0.972	0.003	0.983	0.002	0.913	0.005
	FNR	0.053	0.003	0.111	0.004	0.100	0.005	0.164	0.004
	FPR	0.012	0.001	0.028	0.003	0.017	0.002	0.087	0.005
	TNR	0.988	0.001	0.889	0.004	0.901	0.005	0.836	0.004
	Precision	0.989	0.001	0.897	0.004	0.908	0.005	0.848	0.003

	Recall	0.947	0.003	0.972	0.003	0.983	0.002	0.913	0.005
	F1 score	0.968	0.002	0.933	0.002	0.944	0.003	0.879	0.003
Testing	CAR (%)	95.578	0.438	92.144	0.575	92.714	0.495	87.342	0.776
	TPR	0.932	0.007	0.965	0.006	0.978	0.004	0.911	0.011
	FNR	0.068	0.007	0.122	0.010	0.124	0.010	0.164	0.009
	FPR	0.018	0.003	0.035	0.006	0.022	0.004	0.089	0.011
	TNR	0.982	0.003	0.878	0.010	0.876	0.010	0.836	0.009
	Precision	0.983	0.003	0.888	0.008	0.888	0.008	0.848	0.007
	Recall	0.932	0.007	0.965	0.006	0.978	0.004	0.911	0.011
	F1 score	0.957	0.004	0.925	0.005	0.931	0.005	0.878	0.008

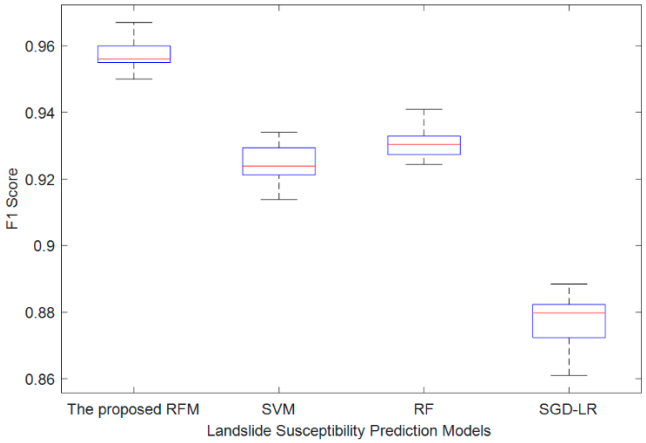

Figure 9. Model performances obtained from the repetitive data sampling process.

Also, the non-parametric Wilcoxon signed-rank test [85] was used to better demonstrate the statistical significance of the difference in model results. A detailed explanation of this test for landslide susceptibility mapping can be found in [43]. In this research, the significant level (*p*-value) of the employed hypothesis test was set to be 0.05. The results of the Wilcoxon signed-rank test performed on the models' F1 score outcomes are reported in Table 4. As shown in this table, with *p*-values <0.05, the null hypothesis of equal means could be confidently rejected and it is possible conclude that that the predictive performances of the landslide prediction models were statistically different. These facts confirmed that the newly developed RFM is highly suited for the spatial prediction of a landslide in the study region.

Table 4. The Wilcoxon signed-rank test results.

Pairwise Model Comparison	*p*-Value	Test Outcome
The proposed RFM vs. SVM	0.0001	Significant
The proposed RFM vs. RF	0.0001	Significant
The proposed RFM vs. SGD-LR	0.0001	Significant

Since the proposed RFM achieved the most desired predictive result with the GIS database collected from the study area, this innovative prediction model was then employed to construct a landslide susceptibility map. The landslide susceptibility map for the study area established by the RFM is demonstrated in Figure 10. To validate the accuracy and helpfulness of the newly created susceptibility map, the landslide inventory map, which showed the locations of the past landslide occurrences, was overlaid with the new map. The graphic curve [86] was then plotted with the percentage of the landslide pixels on the *y*-axis and the percentage of pixels of susceptible classes arranged from high to low susceptible indexes. As can be seen from the graphic curve, most of the actual landslide pixels were located in high and very high classes, whereas very few actual landslide pixels were found to be in low and very low classes. These facts confirm the correctness and applicability of the susceptibility map created by the newly developed RFM model. The MATLAB codes and data of the proposed model in this study are in a github repository, that can be found at https://github.com/NhatDucHoang/RFC_SVC_LandslidePredictionModel.

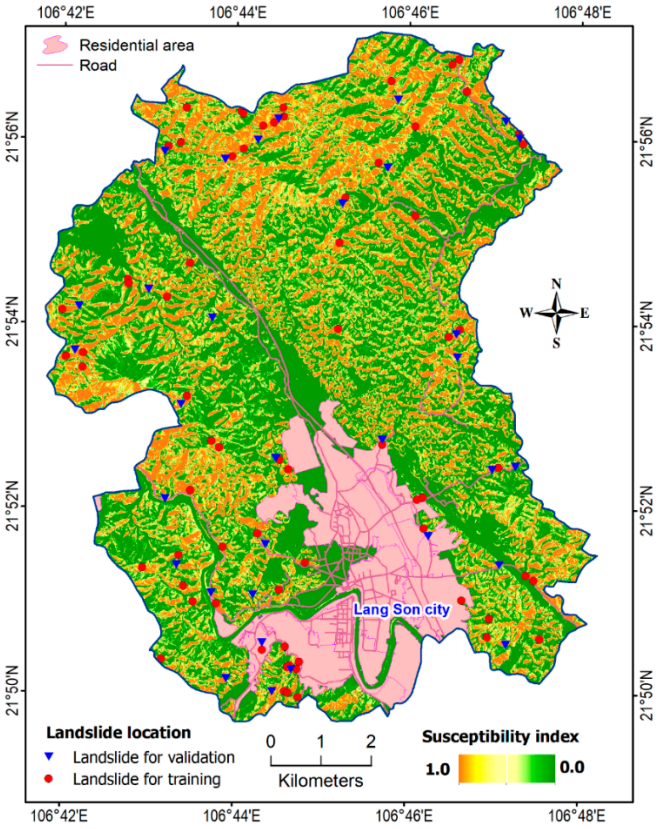

Figure 10. The landslide susceptibility map for the study area derived from the proposed random forest machine model.

6. Conclusions

For land use planning and hazard mitigation, landslide susceptibility evaluation is a crucial task performed by the local authority in mountainous and remote areas in northern Vietnam. These areas have been devastated by natural hazards, including landslides, in recent years due to the combined effects of climate change and human activities (e.g., deforestation). Thus, establishing an updated landslide susceptibility map with better accuracy and reliability is a practical need. To achieve this goal, this study proposed a novel hybrid machine learning framework that employed the RFC and SVM models. The SVM model was integrated into the RFC structure to improve its performance by constructing smooth and flexible class boundaries instead of linear boundaries used by the standard RFC model.

To train and test the capability of the proposed hybrid framework, named as RFM, a GIS database containing information of 101 historical landslide occurrences was used. Experimental results demonstrated that the RFM with an F1 score of roughly 0.96 is superior to other benchmark models of the SVM, RFC, and SGD-LR. Hence, the newly developed ensemble data-driven model can be a helpful tool to assist local authorities in identifying landslide-prone areas so that the task of land use planning can be carried out more effectively. Since the RFM has achieved superior prediction performance for Lang Son city (Vietnam), the proposed hybrid machine learning model has the potential to be applied in other areas outside the study region. Nevertheless, one shortcoming of the current study is that the feature selection method has not been integrated into the model. Therefore, the future extension of this study may include the utilization of more advanced feature selection strategies. Furthermore, the integration of other sophisticated machine learning methods (e.g., the least-squares SVM) with the RFC can be worth investigating.

Author Contributions: Methodology, V.-H.D., N.-D.H., P.S., and L.-M.-D.L.; software, V.-H.D. and N.-D.H; validation, D.T.B., P.S., and N.-D.H.; formal analysis, D.T.B. and N.-D.H.; investigation, D.T.B.; resources, D.T.B.;

writing—original draft preparation, V.-H.D., N.-D.H., and L.-M.-D.L.; writing—review and editing, D.T.B. and P.S. All authors have read and agreed to the published version of the manuscript.

Funding: This research was support by the Geographic Information Science Research Group, Ton Duc Thang University, Ho Chi Minh City, Vietnam (HD. Pijush.Samui-2019) . The APC was funded by University of South-Eastern Norway, Bø i Telemark, Norway.

Conflicts of Interest: The authors declare no conflict of interest.

References

1. WHO. LANDSLIDES—Technical Hazard Sheet—Natural Disaster Profiles. Available online: https://www.who.int/hac/techguidance/ems/landslides/en/ (accessed 5 September 2019).
2. Haque, U.; Da Silva, P.F.; Devoli, G.; Pilz, J.; Zhao, B.; Khaloua, A.; Wilopo, W.; Andersen, P.; Lu, P.; Lee, J.; et al. The human cost of global warming: Deadly landslides and their triggers (1995–2014). *Sci. Total Environ.* **2019**, *682*, 673–684.
3. Hoa, T.X. *Landslide Risks Located in Ten Northern Mountainous Localities*; Institute of Geosciences and Mineral Resources under Ministry of Natural Resources and Environment: Hanoi, Vietnam, 2019.
4. Reichenbach, P.; Rossi, M.; Malamud, B.D.; Mihir, M.; Guzzetti, F. A review of statistically-based landslide susceptibility models. *Earth-Sci. Rev.* **2018**, *180*, 60–91.
5. Hansen, A.; Franks, C.A.M.; Kirk, P.A.; Brimicombe, A.J.; Tung, F. Application of GIS to Hazard Assessment, with Particular Reference to Landslides in Hong Kong. In *Geographical Information Systems in Assessing Natural Hazards*; Carrara, A., Guzzetti, F., Eds.; Springer: Dordrecht, The Netherlands, 1995; pp. 273–298.
6. Montrasio, L.; Valentino, R.; Meisina, C. Soil Saturation and Stability Analysis of a Test Site Slope Using the Shallow Landslide Instability Prediction (SLIP) Model. *Geotech. Geol. Eng.* **2018**, *36*, 2331–2342.
7. Cheng, M.-Y.; Hoang, N.-D. Slope Collapse Prediction Using Bayesian Framework with K-Nearest Neighbor Density Estimation: Case Study in Taiwan. *J. Comput. Civ. Eng.* **2016**, *30*, 04014116.
8. Reichenbach, P.; Galli, M.; Cardinali, M.; Guzzetti, F.; Ardizzone, F. Geomorphological Mapping to Assess Landslide Risk: Concepts, Methods and Applications in the Umbria Region of Central Italy. In *Landslide Hazard and Risk*; John Wiley: Chichester, UK, 2005; pp. 429–468.
9. Mejía-Navarro, M.; Wohl, E.E.; Oaks, S.D. Geological hazards, vulnerability, and risk assessment using GIS: Model for Glenwood Springs, Colorado. *Geomorphology* **1994**, *10*, 331–354.
10. Wang, Y.; Fang, Z.; Hong, H. Comparison of convolutional neural networks for landslide susceptibility mapping in Yanshan County, China. *Sci. Total Environ.* **2019**, *666*, 975–993.
11. Kavzoglu, T.; Colkesen, I.; Sahin, E.K. Machine Learning Techniques in Landslide Susceptibility Mapping: A Survey and a Case Study. In *Landslides: Theory, Practice and Modelling*; Pradhan, S.P., Vishal, V., Singh, T.N., Eds.; Springer International Publishing: Cham, Switzerland, 2019; pp. 283–301.
12. Alvioli, M.; Baum, R.L. Parallelization of the TRIGRS model for rainfall-induced landslides using the message passing interface. *Environ. Model. Softw.* **2016**, *81*, 122–135.
13. Anagnostopoulos, G.G.; Fatichi, S.; Burlando, P. An advanced process-based distributed model for the investigation of rainfall-induced landslides: The effect of process representation and boundary conditions. *Water Resour. Res.* **2015**, *51*, 7501–7523.
14. Montgomery, D.R.; Dietrich, W.E. A physically based model for the topographic control on shallow landsliding. *Water Resour. Res.* **1994**, *30*, 1153–1171.
15. Bui, D.T.; Hoang, N.-D.; Nguyen, H.; Tran, X.-L. Spatial prediction of shallow landslide using Bat algorithm optimized machine learning approach: A case study in Lang Son Province, Vietnam. *Adv. Eng. Inform.* **2019**, *42*, 100978.
16. Pham, B.T.; Jaafari, A.; Prakash, I.; Bui, D.T. A novel hybrid intelligent model of support vector machines and the MultiBoost ensemble for landslide susceptibility modeling. *Bull. Eng. Geol. Environ.* **2019**, *78*, 2865–2886.
17. Park, S.-J.; Lee, C.-W.; Lee, S.; Lee, M.-J. Landslide Susceptibility Mapping and Comparison Using Decision Tree Models: A Case Study of Jumunjin Area, Korea. *Remote Sens.* **2018**, *10*, 1545.
18. Lombardo, L.; Mai, P.M. Presenting logistic regression-based landslide susceptibility results. *Eng. Geol.* **2018**, *244*, 14–24.

19. Polykretis, C.; Chalkias, C.; Ferentinou, M. Adaptive neuro-fuzzy inference system (ANFIS) modeling for landslide susceptibility assessment in a Mediterranean hilly area. *Bull. Eng. Geol. Environ.* **2019**, *78*, 1173–1187.
20. Zhu, A.X.; Miao, Y.; Liu, J.; Bai, S.; Zeng, C.; Ma, T.; Hong, H. A similarity-based approach to sampling absence data for landslide susceptibility mapping using data-driven methods. *Catena* **2019**, *183*, 104188.
21. Aditian, A.; Kubota, T.; Shinohara, Y. Comparison of GIS-based landslide susceptibility models using frequency ratio, logistic regression, and artificial neural network in a tertiary region of Ambon, Indonesia. *Geomorphology* **2018**, *318*, 101–111.
22. Hemasinghe, H.; Rangali, R.S.S.; Deshapriya, N.L.; Samarakoon, L. Landslide susceptibility mapping using logistic regression model (a case study in Badulla District, Sri Lanka). *Procedia Eng.* **2018**, *212*, 1046–1053.
23. Kalantar, B.; Pradhan, B.; Naghibi, S.A.; Motevalli, A.; Mansor, S. Assessment of the effects of training data selection on the landslide susceptibility mapping: A comparison between support vector machine (SVM), logistic regression (LR) and artificial neural networks (ANN). *Geomat. Nat. Hazards Risk* **2018**, *9*, 49–69.
24. Abedini, M.; Ghasemian, B.; Shirzadi, A.; Shahabi, H.; Chapi, K.; Pham, B.T.; Bin Ahmad, B.; Tien Bui, D. A novel hybrid approach of Bayesian Logistic Regression and its ensembles for landslide susceptibility assessment. *Geocarto Int.* **2018**, *34*, 1427–1457.
25. Chen, W.; Xie, X.; Wang, J.; Pradhan, B.; Hong, H.; Bui, D.T.; Duan, Z.; Ma, J. A comparative study of logistic model tree, random forest, and classification and regression tree models for spatial prediction of landslide susceptibility. *Catena* **2017**, *151*, 147–160.
26. Polykretis, C.; Chalkias, C. Comparison and evaluation of landslide susceptibility maps obtained from weight of evidence, logistic regression, and artificial neural network models. *Nat. Hazards* **2018**, *93*, 249–274.
27. Jaafari, A.; Panahi, M.; Pham, B.T.; Shahabi, H.; Bui, D.T.; Rezaie, F.; Lee, S. Meta optimization of an adaptive neuro-fuzzy inference system with grey wolf optimizer and biogeography-based optimization algorithms for spatial prediction of landslide susceptibility. *Catena* **2019**, *175*, 430–445.
28. Ada, M.; San, B.T. Comparison of machine-learning techniques for landslide susceptibility mapping using two-level random sampling (2LRS) in Alakir catchment area, Antalya, Turkey. *Nat. Hazards* **2018**, *90*, 237–263.
29. Alkhasawneh, M.S.; Ngah, U.K.; Tay, L.T.; Isa, N.A.M.; Al-Batah, M.S. Modeling and Testing Landslide Hazard Using Decision Tree. *J. Appl. Math.* **2014**, *2014*, 9.
30. Kadavi, P.R.; Lee, C.-W.; Lee, S. Application of Ensemble-Based Machine Learning Models to Landslide Susceptibility Mapping. *Remote Sens.* **2018**, *10*, 1252.
31. Hong, H.; Liu, J.; Bui, D.T.; Pradhan, B.; Acharya, T.D.; Pham, B.T.; Zhu, A.X.; Chen, W.; Ahmad, B.B. Landslide susceptibility mapping using J48 Decision Tree with AdaBoost, Bagging and Rotation Forest ensembles in the Guangchang area (China). *Catena* **2018**, *163*, 399–413.
32. Nguyen, Q.-K.; Bui, D.T.; Hoang, N.-D.; Trinh, P.T.; Nguyen, V.-H.; Yilmaz, I. A Novel Hybrid Approach Based on Instance Based Learning Classifier and Rotation Forest Ensemble for Spatial Prediction of Rainfall-Induced Shallow Landslides using GIS. *Sustainability* **2017**, *9*, 813.
33. Juliev, M.; Mergili, M.; Mondal, I.; Nurtaev, B.; Pulatov, A.; Hübl, J. Comparative analysis of statistical methods for landslide susceptibility mapping in the Bostanlik District, Uzbekistan. *Sci. Total Environ.* **2019**, *653*, 801–814.
34. Bragagnolo, L.; Silva, R.V.D.; Grzybowski, J.M.V. Artificial neural network ensembles applied to the mapping of landslide susceptibility. *Catena* **2020**, *184*, 104240.
35. Choubin, B.; Abdolshahnejad, M.; Moradi, E.; Querol, X.; Mosavi, A.; Shamshirband, S.; Ghamisi, P. Spatial hazard assessment of the PM10 using machine learning models in Barcelona, Spain. *Sci. Total Environ.* **2020**, *701*, 134474.
36. Choubin, B.; Mosavi, A.; Alamdarloo, E.H.; Hosseini, F.S.; Shamshirband, S.; Dashtekian, K.; Ghamisi, P. Earth fissure hazard prediction using machine learning models. *Environ. Res.* **2019**, *179*, 108770.
37. Choubin, B.; Borji, M.; Mosavi, A.; Sajedi-Hosseini, F.; Singh, V.P.; Shamshirband, S. Snow avalanche hazard prediction using machine learning methods. *J. Hydrol.* **2019**, *577*, 123929.
38. Rahmati, O.; Ghorbanzadeh, O.; Teimurian, T.; Mohammadi, F.; Tiefenbacher, J.P.; Falah, F.; Pirasteh, S.; Ngo, P.T.T.; Bui, D.T. Spatial Modeling of Snow Avalanche Using Machine Learning Models and Geo-Environmental Factors: Comparison of Effectiveness in Two Mountain Regions. *Remote Sens.* **2019**, *11*, 2995.

39. Rahmati, O.; Yousefi, S.; Kalantari, Z.; Uuemaa, E.; Teimurian, T.; Keesstra, S.; Pham, T.D.; Tien Bui, D. Multi-hazard exposure mapping using machine learning techniques: A case study from Iran. *Remote Sens.* **2019**, *11*, 1943.
40. Rahmati, O.; Choubin, B.; Fathabadi, A.; Coulon, F.; Soltani, E.; Shahabi, H.; Mollaefar, E.; Tiefenbacher, J.; Cipullo, S.; Ahmad, B.B.; et al. Predicting uncertainty of machine learning models for modelling nitrate pollution of groundwater using quantile regression and UNEEC methods. *Sci. Total Environ.* **2019**, *688*, 855–866.
41. Bui, D.T.; Hoang, N.D.; Martínez-Álvarez, F.; Ngo, P.T.T.; Hoa, P.V.; Pham, T.D.; Samui, P.; Costache, R. A novel deep learning neural network approach for predicting flash flood susceptibility: A case study at a high frequency tropical storm area. *Sci. Total Environ.* **2020**, *701*, 134413.
42. Bui, D.T.; Hoang, N.D.; Pham, T.D.; Ngo, P.T.T.; Hoa, P.V.; Minh, N.Q.; Tran, X.T.; Samui, P. A new intelligence approach based on GIS-based Multivariate Adaptive Regression Splines and metaheuristic optimization for predicting flash flood susceptible areas at high-frequency tropical typhoon area. *J. Hydrol.* **2019**, *575*, 314–326.
43. Tien Bui, D.; Tsangaratos, P.; Nguyen, V.T. ; Van Liem, N. ;Trinh, P.T.. Comparing the prediction performance of a Deep Learning Neural Network model with conventional machine learning models in landslide susceptibility assessment. *Catena* **2019**, *188*, 104426.
44. Dou, J.; Yunus, A.P.; Bui, D.T.; Merghadi, A.; Sahana, M.; Zhu, Z.; Chen, C.W.; Khosravi, K.; Yang, Y.; Pham, B.T. Assessment of advanced random forest and decision tree algorithms for modeling rainfall-induced landslide susceptibility in the Izu-Oshima Volcanic Island, Japan. *Sci. Total Environ.* **2019**, *662*, 332–346.
45. Ho, T.K. Random decision forests. In Proceedings of the 3rd International Conference on Document Analysis and Recognition, Montreal, QC, Canada, 14–16 August 1995; Volume 1, pp. 278–282.
46. Breiman, L. Random Forests. *Mach. Learn.* **2001**, *45*, 5–32.
47. Vapnik, V.N. *Statistical Learning Theory*; John Wiley & Sons, Inc.: New York, NY, USA, 1998; ISBN 0471030031.
48. Boser, B.E.; Guyon, I.M.; Vapnik, V.N. A training algorithm for optimal margin classifiers. In Proceedings of the Fifth Annual Workshop on Computational Learning Theory, Pittsburgh, PA, USA, 27–29 July 1992.
49. Dang, V.-H.; Dieu, T.B.; Tran, X.-L.; Hoang, N.-D. Enhancing the accuracy of rainfall-induced landslide prediction along mountain roads with a GIS-based random forest classifier. *Bull. Eng. Geol. Environ.* **2018**, *78*, 2835–2849.
50. Chen, W.; Pourghasemi, H.R.; Naghibi, S.A. A comparative study of landslide susceptibility maps produced using support vector machine with different kernel functions and entropy data mining models in China. *Bull. Eng. Geol. Environ.* **2008**, *77*, 647–664.
51. Huang, Y.; Zhao, L. Review on landslide susceptibility mapping using support vector machines. *Catena* **2018**, *165*, 520–529.
52. Tien Bui, D.; Shahabi, H.; Shirzadi, A.; Chapi, K.; Hoang, N.D.; Pham, B.; Bui, Q.T.; Tran, C.T.; Panahi, M.; Bin Ahamd, B.; et al. A Novel Integrated Approach of Relevance Vector Machine Optimized by Imperialist Competitive Algorithm for Spatial Modeling of Shallow Landslides. *Remote Sens.* **2018**, *10*, 1538.
53. Tam, V.T.; Tuy, P.K.; Nam, N.X.; Tuan, L.C.; Tuan, N.D.; Trung, N.D.; Thang, D.V.; Ha, P.V. *Geohazard Investigation in Some Key Areas of the Northern Mountainous Area of Vietnam for the Planning of Socio-Economic Development Vietnam*; Technical Report; Institute of Geosciences and Mineral Resources: Hanoi, Vietnam, 2006; Volume 83, pp. 56–62.
54. Hearn, G.J.; Hart, A.B. Landslide susceptibility mapping: A practitioner's view. *Bull. Eng. Geol. Environ.* **2019**, doi:10.1007/s10064-019-01506-1.
55. Pham, B.T.; Bui, D.T.; Pourghasemi, H.R.; Indra, P.; Dholakia, M.B. Landslide susceptibility assesssment in the Uttarakhand area (India) using GIS: A comparison study of prediction capability of naïve bayes, multilayer perceptron neural networks, and functional trees methods. *Theor. Appl. Climatol.* **2017**, *128*, 255–273.
56. Chen, W.; Panahi, M.; Pourghasemi, H.R. Performance evaluation of GIS-based new ensemble data mining techniques of adaptive neuro-fuzzy inference system (ANFIS) with genetic algorithm (GA), differential evolution (DE), and particle swarm optimization (PSO) for landslide spatial modelling. *Catena* **2017**, *157*, 310–324.

57. North, M.A. A Method for Implementing a Statistically Significant Number of Data Classes in the Jenks Algorithm. In Proceedings of the Sixth International Conference on Fuzzy Systems and Knowledge Discovery, Tianjin, China, 14–16 August 2009; Volume 1, pp. 35–38.
58. Hung, L.; Van, N.; Duc, D.; Ha, L.; Son, P.; Khanh, N.; Binh, L. Landslide susceptibility mapping by combining the analytical hierarchy process and weighted linear combination methods: A case study in the upper Lo River catchment (Vietnam). *Landslides* **2016**, *13*, 1285–1301.
59. Robnik-Šikonja, M.; Kononenko, I. Theoretical and Empirical Analysis of ReliefF and RReliefF. *Mach. Learn.* **2003**, *53*, 23–69.
60. Kuncheva, L.I. *Combining Pattern Classifiers: Methods and Algorithms*; John Wiley & Sons, Inc.: New York, NY, USA, 2014.
61. Kleinberg, E.M. Stochastic discrimination. *Ann. Math. Artif. Intell.* **1990**, *1*, 207–239.
62. Arabameri, A.; Yamani, M.; Pradhan, B.; Melesse, A.; Shirani, K.; Bui, D.T. Novel ensembles of COPRAS multi-criteria decision-making with logistic regression, boosted regression tree, and random forest for spatial prediction of gully erosion susceptibility. *Sci. Total Environ.* **2019**, *688*, 903–916.
63. Li, Z.; Cheng, C.; Kwan, M.-P.; Tong, X.; Tian, S. Identifying Asphalt Pavement Distress Using UAV LiDAR Point Cloud Data and Random Forest Classification. *ISPRS Int. J. Geo-Inf.* **2019**, *8*, 39.
64. Sun, Z.; Sun, H.; Zhang, J. Multistep Wind Speed and Wind Power Prediction Based on a Predictive Deep Belief Network and an Optimized Random Forest. *Math. Probl. Eng.* **2018**, *2018*, 15.
65. Kim, J.-C.; Lee, S.; Jung, H.-S.; Lee, S. Landslide susceptibility mapping using random forest and boosted tree models in Pyeong-Chang, Korea. *Geocarto Int.* **2018**, *33*, 1000–1015.
66. Trigila, A.; Iadanza, C.; Esposito, C.; Scarascia-Mugnozza, G. Comparison of Logistic Regression and Random Forests techniques for shallow landslide susceptibility assessment in Giampilieri (NE Sicily, Italy). *Geomorphology* **2015**, *249*, 119–136.
67. Chen, W.; Xie, X.; Peng, J.; Shahabi, H.; Hong, H.; Bui, D.T.; Duan, Z.; Li, S.; Zhu, A.X. GIS-based landslide susceptibility evaluation using a novel hybrid integration approach of bivariate statistical based random forest method. *Catena* **2018**, *164*, 135–149.
68. Rokach, L.; Maimon, O. *Datamining and Knowledge Discovery Handbook*; Springer: Boston, MA, USA, 2010.
69. Bonissone, P.; Cadenas, J.M.; Garrido, M.C.; Díaz-Valladares, R.A. A fuzzy random forest. *Int. J. Approx. Reason.* **2010**, *51*, 729–747.
70. Tehrany, M.S.; Pradhan, B.; Mansor, S.; Ahmad, N. Flood susceptibility assessment using GIS-based support vector machine model with different kernel types. *Catena* **2015**, *125*, 91–101.
71. Sachdeva, S.; Bhatia, T.; Verma, A.K. Flood susceptibility mapping using GIS-based support vector machine and particle swarm optimization: A case study in Uttarakhand (India). In Proceedings of the 2017 8th International Conference on Computing, Communication and Networking Technologies (ICCCNT), Delhi, India, 3–5 July 2017; pp. 1–7.
72. Deo, R.C.; Kisi, O.; Singh, V.P. Drought forecasting in eastern Australia using multivariate adaptive regression spline, least square support vector machine and M5Tree model. *Atmos. Res.* **2017**, *184*, 149–175.
73. Choubin, B.; Moradi, E.; Golshan, M.; Adamowski, J.; Sajedi-Hosseini, F.; Mosavi, A. An Ensemble prediction of flood susceptibility using multivariate discriminant analysis, classification and regression trees, and support vector machines. *Sci. Total Environ.* **2019**, *651*, 2087–2096.
74. Yao, X.; Tham, L.; Dai, F. Landslide susceptibility mapping based on support vector machine: A case study on natural slopes of Hong Kong, China. *Geomorphology* **2008**, *101*, 572–582.
75. Pradhan, B. A comparative study on the predictive ability of the decision tree, support vector machine and neuro-fuzzy models in landslide susceptibility mapping using GIS. *Comput. Geosci.* **2013**, *51*, 350–365.
76. Hoang, N.-D.; Nguyen, Q.-L.; Bui, D.T. Image Processing-Based Classification of Asphalt Pavement Cracks Using Support Vector Machine Optimized by Artificial Bee Colony. *J. Comput. Civ. Eng.* **2018**, *32*, 04018037.
77. Hoang, N.-D.; Bui, D.T. Predicting earthquake-induced soil liquefaction based on a hybridization of kernel Fisher discriminant analysis and a least squares support vector machine: A multi-dataset study. *Bull. Eng. Geol. Environ.* **2018**, *77*, 191–204.
78. Bui, D.T.; Tuan, A.T.; Klempe, H.; Pradhan, B.; Revhaug, I. Spatial prediction models for shallow landslide hazards: A comparative assessment of the efficacy of support vector machines, artificial neural networks, kernel logistic regression, and logistic model tree. *Landslides* **2016**, *13*, 361–378.

79. Pham, B.T.; Pradhan, B.; Bui, D.T.; Prakash, I.; Dholakia, M. A comparative study of different machine learning methods for landslide susceptibility assessment: A case study of Uttarakhand area (India). *Environ. Model. Softw.* **2016**, *84*, 240–250.
80. Joshi, P.P.; Wynne, R.H.; Thomas, V.A. Cloud detection algorithm using SVM with SWIR2 and tasseled cap applied to Landsat 8. *Int. J. Appl. Earth Obs. Geoinf.* **2019**, *82*, 101898.
81. Sokolova, M.; Japkowicz, N.; Szpakowicz, S. Beyond accuracy, F-score and ROC: A family of discriminant measures for performance evaluation. In Proceedings of the Australasian Joint Conference on Artificial Intelligence, Hobart, Australia, 4–8 December 2006; Springer: Berlin/Heidelberg, Germany, 2006; pp. 1015–1021.
82. Sasaki, Y. The truth of the F-measure. *Teach Tutor Mater* **2007**, *26*, 1–5. Available online: https://www.cs.odu.edu/~mukka/cs795sum09dm/Lecturenotes/Day3/F-measure-YS-26Oct07.pdf (accessed on 30 December 2019).
83. Wang, L.-J.; Guo, M.; Sawada, K.; Lin, J.; Zhang, J. A comparative study of landslide susceptibility maps using logistic regression, frequency ratio, decision tree, weights of evidence and artificial neural network. *Geosci. J.* **2016**, *20*, 117–136.
84. Matwork. *Statistics and Machine Learning Toolbox User's Guide*; Matwork Inc.: Natick, MA, USA, 2017. Available online: https://www.mathworks.com/help/pdf_doc/stats/stats.pdf (accessed on 4 August 2018).
85. Hollander, M.; Wolfe, D.A. *Nonparametric Statistical Methods*; John Wiley & Sons: Hoboken, NJ, USA, 1999.
86. Chung, C.-J.F.; Fabbri, A.G.; van Westen, C.J. Multivariate regression analysis for landslide hazard zonation. In *Geographical Information Systems in Assessing Natural Hazards*; Springer: Dordrecht, The Netherlands, 1995; pp. 107–133.